Electronic Supplementary Information

Insight into the plasmonic "hot spots" and efficient hot electron injection induced by Ag nanoparticles in a covalent organic framework for photocatalytic H_2 evolution

Lihua Zhang [a,b], Xu Lu [a], Jiaqi Sun [a,b], Cunxia Wang [a,b], Pengyu Dong [a,*]

[a] Key Laboratory for Advanced Technology in Environmental Protection of Jiangsu Province, Yancheng Institute of Technology, Yancheng 224051, P. R. China.

[b] School of Mechanical Engineering, Yancheng Institute of Technology, Yancheng 224051, P. R. China

* Corresponding authors.

E-mail address: dongpy11@gmail.com (P. Dong).

1. Supplementary Figures

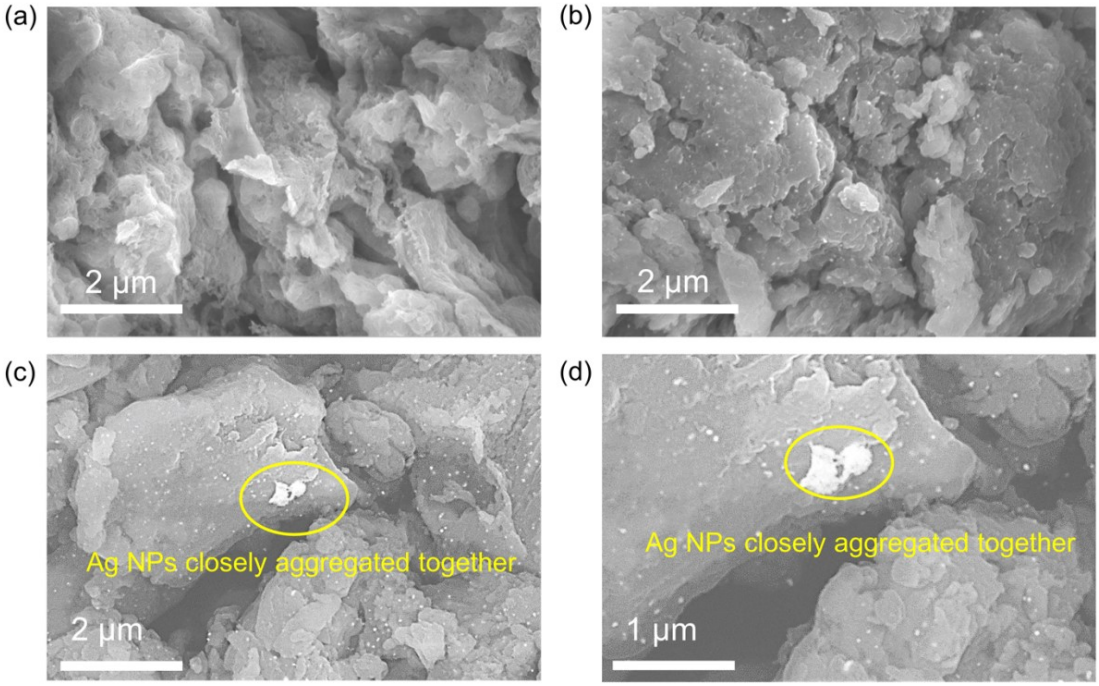

Fig. S1. SEM images of (a) TpPa-1-COF, (b) 3% Ag/TpPa-1, and (c, d) 5% Ag/TpPa-1.

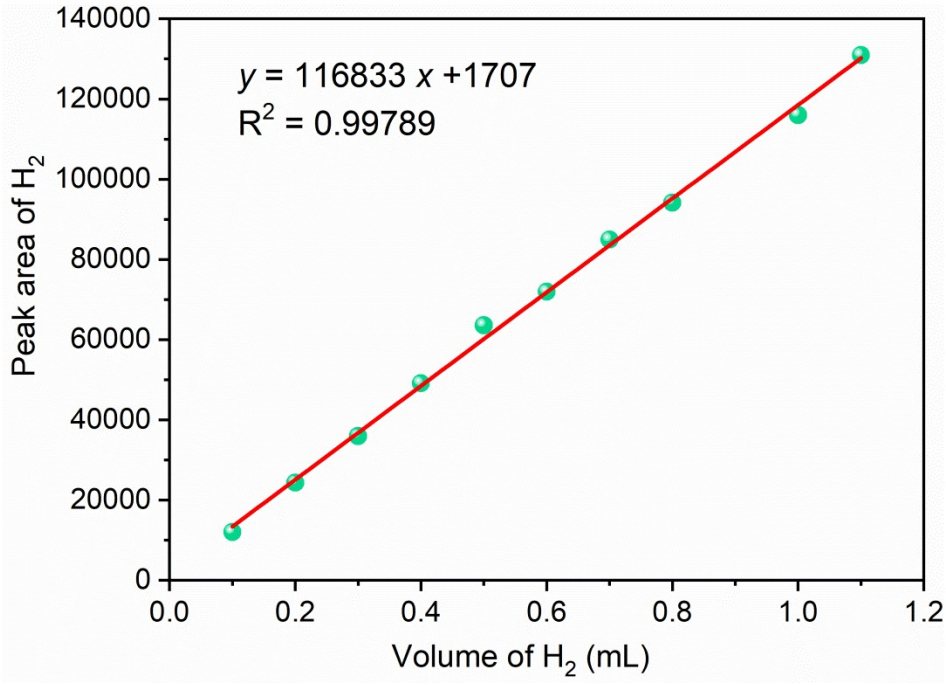

Fig. S2. The standard curve of H_2 production.

We quantify H_2 by the "external standard method" with the help of a standard curve. The standard curve is the trend line of the peak area with the volume/amount of the substance to be measured. After injecting 0.1 ml of high-purity H_2 into the photolytic water reaction system, the peak area S_{A1} can be obtained on the gas chromatography, and then injecting a known volume of 0.1 mL of high-purity H_2 into the photolytic water reaction system (cumulative injection), the peak areas S_{A2}, S_{A3}, S_{A4}, and S_{A5} can be obtained respectively. After linear fitting, the standard curve can be obtained. The standard calibration curve of H_2 detection is shown in Fig. S3. According to the fitted standard curve, the relationship between the peak area and the volume of H_2 evolved can be expressed as Equation S1.

$$y = 116833x + 1707 \quad \text{(S1)}$$

where y is the peak area corresponding to H_2 in the chromatography and x is the volume of H_2 (mL).

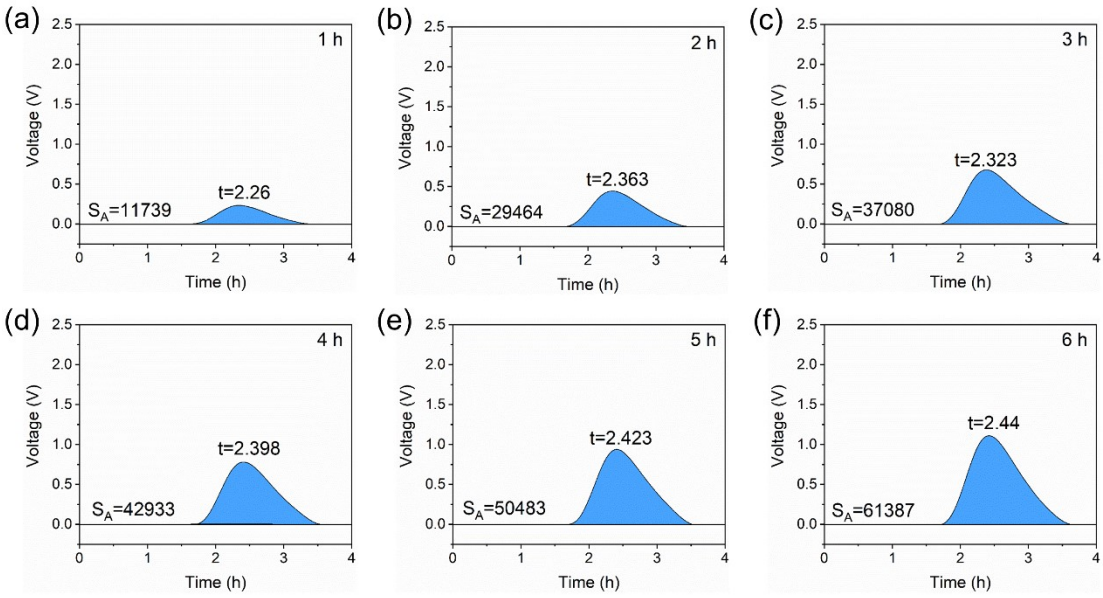

Fig. S3. The chromatogram of H_2 evolved over TpPa-1-COF.

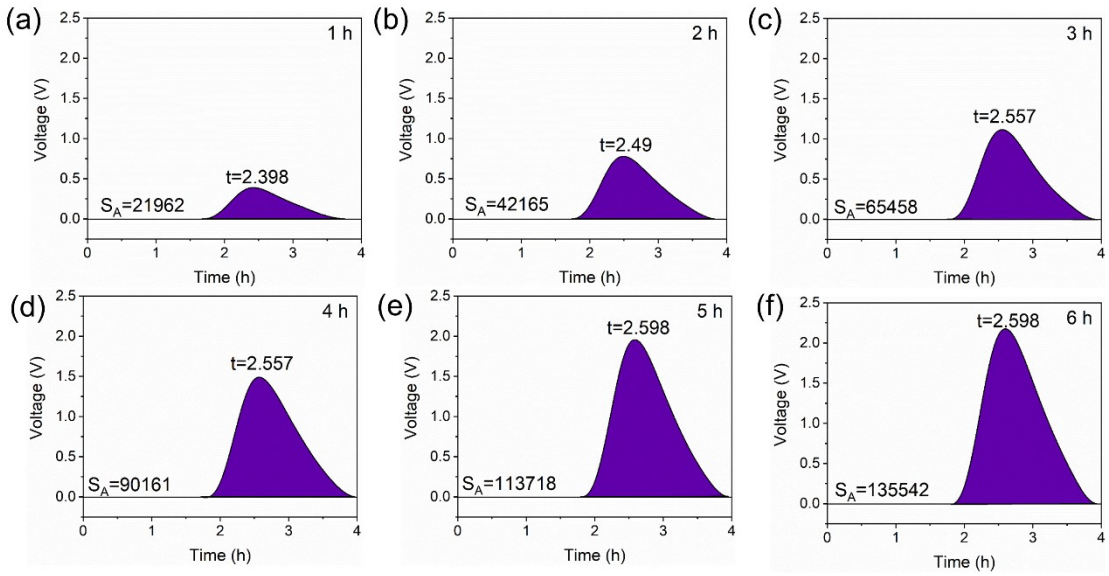

Fig. S4. The chromatogram of H_2 evolved over 3% Ag/TpPa-1.

The volume of H_2 produced by the photolytic water reaction can be calculated by substituting the peak area measured by the photolytic water experiment according to the standard curve. An example of the H_2 evolved chromatogram is given in Fig. S5, which illustrates the process of the peak area over 3% Ag/TpPa-1 photocatalyst under visible light irradiation. The amount of H_2 evolved was determined at an interval of 1 h using an online gas chromatograph instrument with a thermal conductivity detector. The measured peak area was converted into the H_2 evolution rate according to the standard curve (Equation S1).

The number of generated moles (μmol) of H_2 generated can be expressed as Equation S2.

$$n = \frac{V}{22.4} \tag{S2}$$

where n is the number of moles (μmol) of H_2 produced, V is the hydrogen volume evolved (mL), and 22.4 is the molar volume of the gas (mL μmol^{-1}).

Moreover, the number of moles of hydrogen produced per mass of photocatalyst

(μmol g^{-1}) can be expressed as Equation S3:

$$C(\mathrm{H_2}) = \frac{n}{m} \tag{S3}$$

where $C(\mathrm{H_2})$ is the number of moles of hydrogen produced per mass of photocatalyst (μmol g^{-1}) and m is the amount of photocatalyst (g) added in the photocatalytic reactor.

Furthermore, the mean value of the amount of H_2 produced per unit mass of photocatalyst and per unit time (μmol g^{-1} h^{-1}) can be evaluated according to Equation S4−S5.

$$P(\mathrm{H_2}) = \frac{C(\mathrm{H_2})}{t} \tag{S4}$$

$$\bar{P}(\mathrm{H_2}) = \frac{\sum_{i=1}^{n=6} P_i(\mathrm{H_2})}{n} \tag{S5}$$

where P is the amount of H_2 produced per gram of photocatalyst per hour (μmol g^{-1} h^{-1}) and $\bar{P}$ is the mean value of P (μmol g^{-1} h^{-1}).

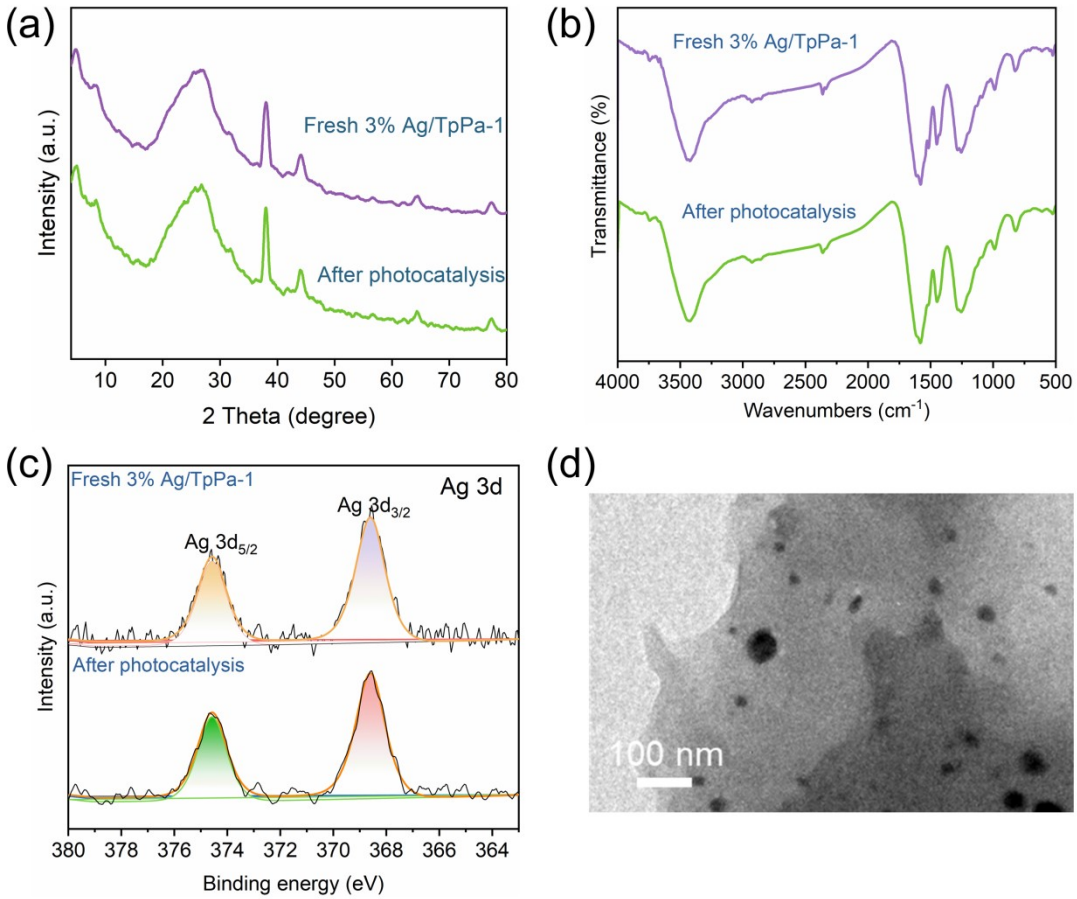

Fig. S5. A comparison of (a) XRD pattern, (b) FTIR spectrum, (c) XPS spectrum, and (d) TEM image of 3% Ag/TpPa-1 before and after photocatalysis.

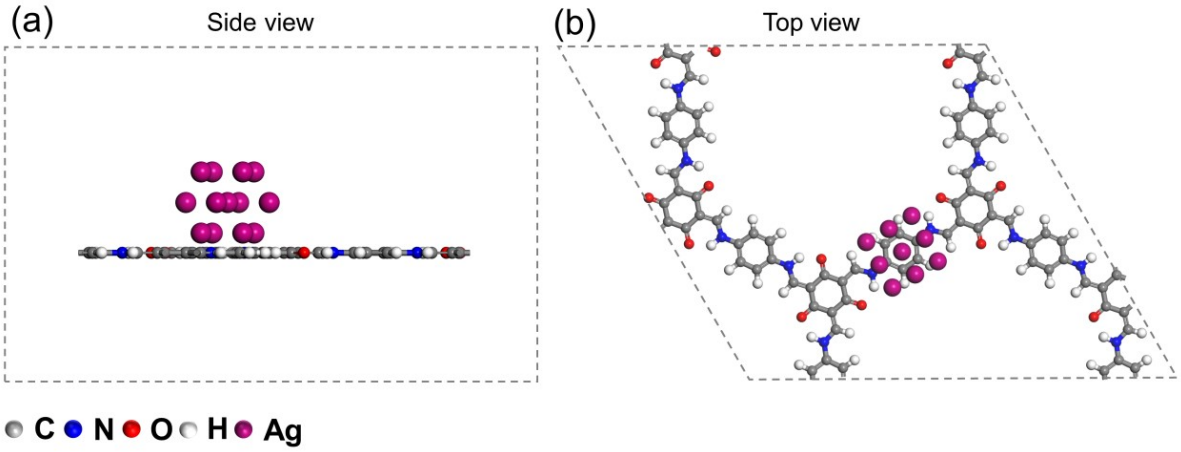

Fig. S6. The constructed geometry model consisted of one unit cell of the TpPa-1-COF (001) plane and an Ag13 cluster from (a) side view and (b) top view.

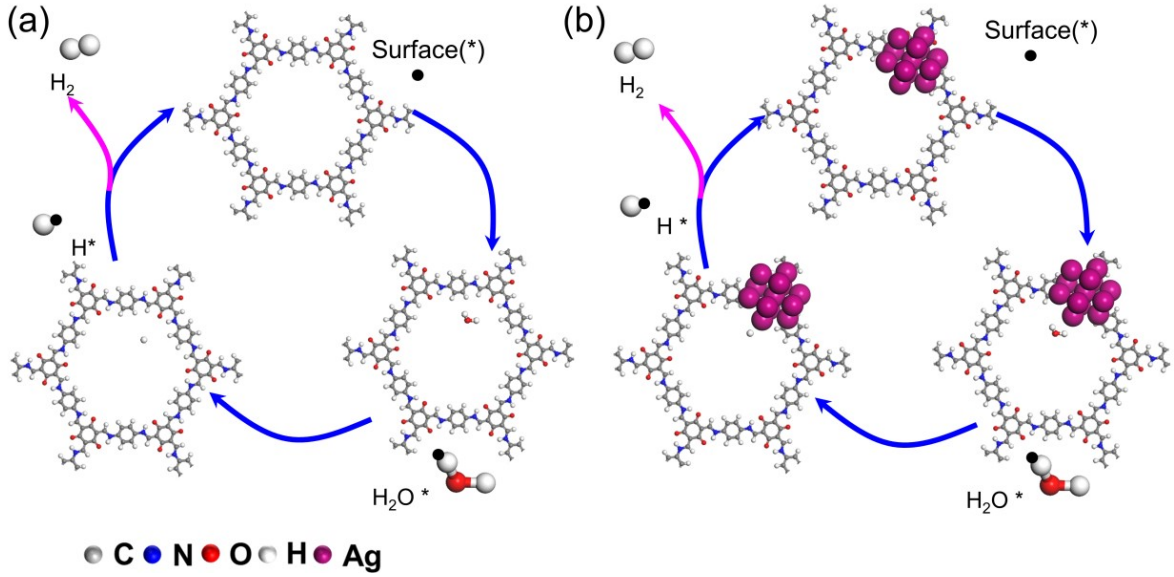

Fig. S7. H_2 evolution process over (a) TpPa-1-COF and (b) Ag/TpPa-1.

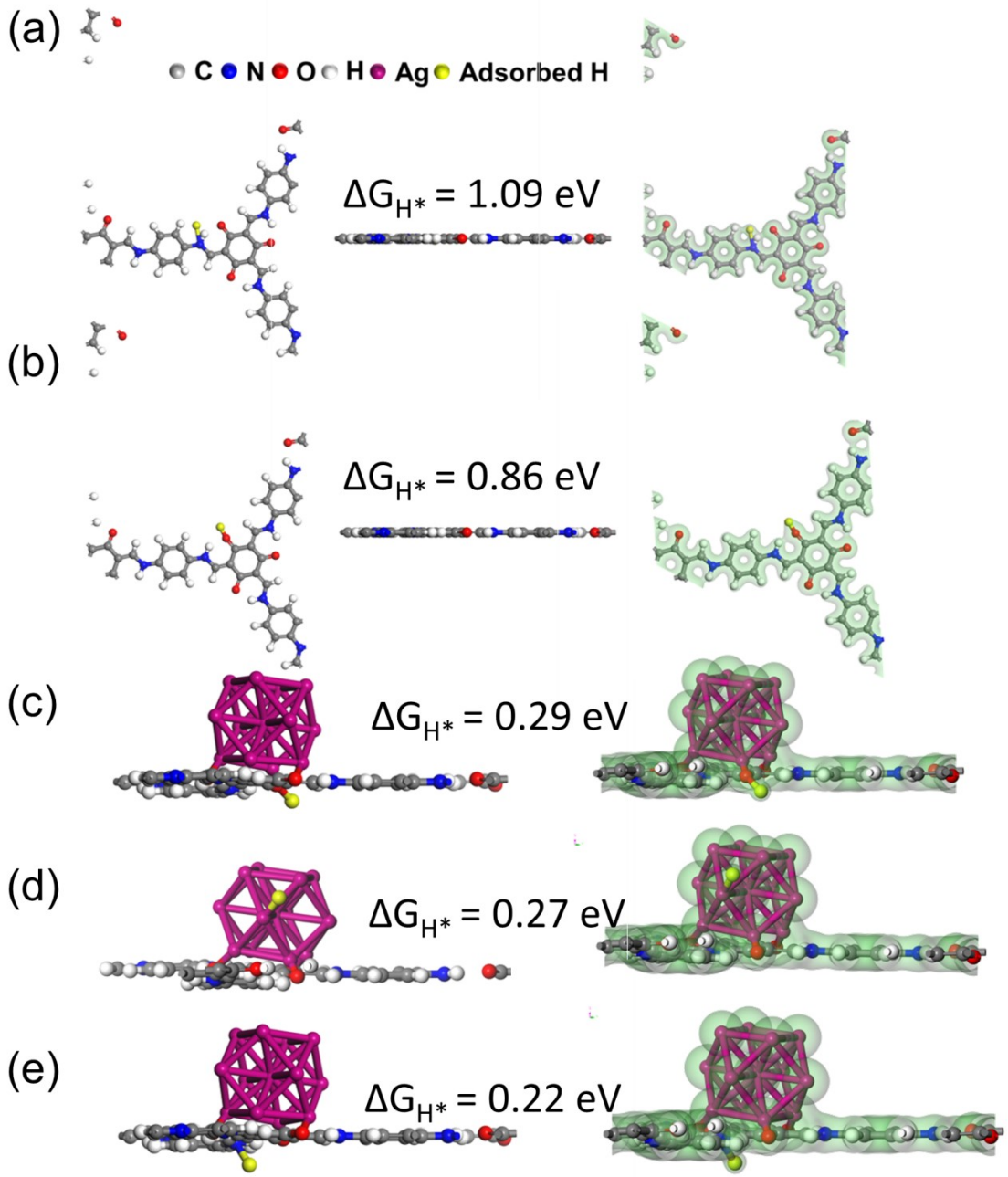

Fig. S8 Atomic structures and the corresponding charge densities of these structures with one H atom adsorbed on (a) N site in TpPa-1, (b) O site in TpPa-1, (c) O site in Ag/TpPa-1, (d) Ag site in Ag/TpPa-1, and (e) N site in Ag/TpPa-1.

2. Supplementary Tables

Table S1. Structural parameters obtained from the Ag L_3-edge EXAFS fitting.

Sample	Shell	[a]N	[b]R(Å)	[c]σ^2 (Å^2)	[d]ΔE_0 (eV)	R, %
Ag foil	Ag−Ag	12	2.88±0.01	0.0100	1.97±0.37	0.0074
	Ag−O	2	2.36±0.01	0.0020		
Ag/TpPa-1	Ag−O	2	2.86±0.01	0.0017	−8.06±1.52	0.0120
	Ag−Ag	4	3.25±0.01	0.0088		

[a]N: numbers for coordination, [b]R: bond distance, [c]σ^2: Debye−Waller factors, [d]ΔE_0: the inner potential correction, R factor (%): degree of the fitting. Based on the experimental EXAFS fitting of the reference Ag foil, S_0^2 was determined to be 1.0 by fixing N as the known crystallographic value. The estimated error boundaries, or accuracy, were N, ±5%, and R, ±1%.

Athena (version 0.9.26) software was used to perform background, pre-edge line, and post-edge line calibrations on the collected XAFS data. After that, a Fourier-transformed fitting was done. For each fitting, the k range of 3−12 Å^{-1} and the R range of 1.4−3.0 Å were used, along with the k^3 weighting. Without any fixed, limited, or correlated variables, the four parameters (N, R, σ^2, and ΔE_0) − coordination number, bond length, Debye−Waller factor, and E_0 shift were fitted.

The $\chi(k)$ obtained by Athena was loaded into the Hama Fortran code for Wavelet Transform analysis. The following parameters were specified: k range = 0−12 Å^{-1}, k weight = 3, R range = 1−4 Å, and a mother Morlet function with κ = 10 and σ = 1.

Table S2. An overview of the H_2 evolution activity in some COFs-based and Ag-related photocatalytic systems.

Photocatalyst	**Co-catalyst**	**Sacrificial agent**	**Solvent**	**Illumination**	**Activity (μmol g^{-1} h^{-1})**	**AQE (%)**	**Ref.**
3% Ag/TpPa-1	–	Ascorbic acid	H_2O	≥ 420 nm	801	1.2（450nm）	This work
3% Pt_1@TpPa-1-COF	–	Sodium ascorbate	PBS	≥ 420 nm	719	0.38 (420 nm)	[1]
MS-c@TpPa-1 (0.3:1)	–	Sodium ascorbate	PBS	≥420 nm	528	0.54 (420 nm)	[2]
α-Fe_2O_3/TpPa-2-COF (3:7)	–	Sodium ascorbate	PBS	≥ 420 nm	3770	0.137 (450 nm)	[3]
CTF-HUST-2	3 wt% Pt	TEOA	H_2O	≥ 420 nm	2647	–	[4]
N_0-COF	Pt	TEOA	PBS	≥ 420 nm	23	–	[5]
N_1-COF	Pt	TEOA	PBS	≥ 420 nm	90	0.075 (450 nm)	[5]
N_2-COF	Pt	TEOA	PBS	≥ 420 nm	438	0.18 (450 nm)	[5]
N_3-COF	Pt	TEOA	PBS	≥ 420 nm	1703	0.44 (450 nm)	[5]
TP-BDDA	Pt	TEOA	H_2O	≥ 395 nm	324	1.3 (420 nm)	[6]
TP-EDDA	Pt	TEOA	H_2O	≥ 395 nm	30	–	[6]
COF-42	Co-1[a]	TEOA	ACN/H_2O	AM 1.5	233	–	[7]
Co_1-phosphide/PCN		None	H_2O	≥ 300 nm	410	3.6 (420 nm)	[8]
ZnPor-DETH-COF	8 wt% Pt	TEOA	PBS	≥ 400 nm	413	0.063 (450 nm)	[9]
g-$C_{18}N_3$-COF	3 wt% Pt	AA	H_2O	≥ 420 nm	292	1.06 (420 nm)	[10]
TpDTz	NiME cluster	TEOA	H_2O	AM 1.5	941	0.2 (400 nm)	[11]
TFA-COF	Pt	TEOA	H_2O	Full wavelength	80	–	[12]
COF-alkene	3 wt% Pt	TEOA	H_2O	≥ 420 nm	2330	6.7 (420 nm)	[13]
COF-imide	3 wt%	TEOA	H_2O	≥ 420 nm	34	–	[13]

Photocatalyst	Co-catalyst	Sacrificial agent	Solvent	Illumination	Activity (μmol g^{-1} h^{-1})	AQE (%)	Ref.
COF-imine	Pt 3 wt% Pt	TEOA	H_2O	≥ 420 nm	12	–	[13]
5% Ag-g-C_3N_4	–	TEOA	H_2O	≥420 nm	586.9	–	[14]
Ag/SnO_2	–	TEOA	H_2O	≥420 nm	700	7.8 (420 nm)	[15]
Ag/TNF 1%	–		H_2O	≥420 nm	146.7	1.3 (420 nm)	[16]
PI/Ag-1	–	Methanol	H_2O	≥420 nm	166	–	[17]
Ag@N/O-C	–	TEOA	H_2O	AM 1.5	44.9	–	[18]
AgNS-CdS	–	Na_2SO_3	H_2O	> 400 nm	341	–	[19]
rGO-AgBr/Ag	–	TEOA	H_2O	AM 1.5	72.71	2.38%	[20]
Ag/SnO_2/C_3N_4	–	Methanol	H_2O	≥420 nm	270	–	[21]
Ag/CQDs/g-C_3N_4	–	TEOA	H_2O	≥400 nm	626.93	–	[22]
Ag/PANI/3DOMM-TiO_{2-x}	–	Methanol	H_2O	AM 1.5	420.90	–	[23]
Ag/N-TiO_{2-x}	–	Methanol	H_2O	AM1.5	186.2	–	[24]
Ag/S-TiO_{2-x}	–	-	H_2O	AM1.5	209.2	–	[25]
Ag/g-C_3N_4	1.0 wt% Pt	TEOA	H_2O	≥420 nm	625	–	[26]
Ag/ND/g-C_3N_4	–	TEOA	H_2O	≥420 nm	158	–	[27]
Ag_2S/KCN-5	0.37 wt% Pt	CH_3OH	H_2O	≥420 nm	96	–	[28]
Ag/$Ag_2Ta_4O_{11}$/ g-C_3N_4	–	TEOA	H_2O	≥420 nm	100.44	–	[29]

References

1. P. Dong, Y. Wang, A. Zhang, T. Cheng, X. Xi and J. Zhang, *ACS Catal.*, 2021, **11**, 13266-13279.
2. Y. Wang, P. Dong, K. Zhu, A. Zhang, J. Pan, Z. Chen, Z. Li, R. Guan, X. Xi and J. Zhang, *Chem. Eng. J.*, 2022, **446**, 136883.
3. Y.-P. Zhang, H.-L. Tang, H. Dong, M.-Y. Gao, C.-C. Li, X.-J. Sun, J.-Z. Wei, Y. Qu, Z.-J. Li and F.-M. Zhang, *J. Mater. Chem. A*, 2020, **8**, 4334-4340.
4. K. Wang, L.-M. Yang, X. Wang, L. Guo, G. Cheng, C. Zhang, S. Jin, B. Tan and A. Cooper, *Angew. Chem. Int. Ed.*, 2017, **56**, 14149-14153.
5. V. S. Vyas, F. Haase, L. Stegbauer, G. Savasci, F. Podjaski, C. Ochsenfeld and B. V. Lotsch, *Nat. Commun.*, 2015, **6**, 8508.
6. P. Pachfule, A. Acharjya, J. Roeser, T. Langenhahn, M. Schwarze, R. Schomacker, A. Thomas and J. Schmidt, *J. Am. Chem. Soc.*, 2018, **140**, 1423-1427.
7. T. Banerjee, F. Haase, G. Savasci, K. Gottschling, C. Ochsenfeld and B. V. Lotsch, *J. Am. Chem. Soc.*, 2017, **139**, 16228-16234.
8. W. Liu, L. Cao, W. Cheng, Y. Cao, X. Liu, W. Zhang, X. Mou, L. Jin, X. Zheng, W. Che, Q. Liu, T. Yao and S. Wei, *Angew. Chem. Int. Ed.*, 2017, **56**, 9312-9317.
9. R. Chen, Y. Wang, Y. Ma, A. Mal, X. Y. Gao, L. Gao, L. Qiao, X. B. Li, L. Z. Wu and C. Wang, *Nat. Commun.*, 2021, **12**, 1354-1363.
10. S. Wei, F. Zhang, W. Zhang, P. Qiang, K. Yu, X. Fu, D. Wu, S. Bi and F. Zhang, *J. Am. Chem. Soc.*, 2019, **141**, 14272-14279.
11. B. P. Biswal, H. A. Vignolo-Gonzalez, T. Banerjee, L. Grunenberg, G. Savasci, K. Gottschling, J. Nuss, C. Ochsenfeld and B. V. Lotsch, *J. Am. Chem. Soc.*, 2019, **141**, 11082-11092.
12. C. Liu, Y. Xiao, Q. Yang, Y. Wang, R. Lu, Y. Chen, C. Wang and H. Yan, *Appl. Surf. Sci.*, 2021, **537**, 148082.
13. C. Mo, M. Yang, F. Sun, J. Jian, L. Zhong, Z. Fang, J. Feng and D. Yu, *Adv. Sci.*, 2020, **7**, 1902988.

14. T. Ren, Y. Dang, Y. Xiao, Q. Hu, D. Deng, J. Chen and P. He, *Inorg. Chem. Commun.* , 2021, **123**, 108367.
15. M. Q. Wang, Y. Liu, M. Zheng and X. Zhou, *Colloids Surf. A Physicochem. Eng. Asp.*, 2022, **650**, 129577.
16. W. L. Zhong, C. Wang, S. L. Peng, R. Y. Shu, Z. P. Tian, Y. P. Du and Y. Chen, *Int. J. Hydrog. Energy*, 2022, **47**, 16507-16517.
17. X. F. Zhao, X. B. Yi, X. Q. Wang, W. Chu, S. P. Guo, J. Zhang, B. X. Liu and X. C. Liu, *Appl. Surf. Sci.*, 2020, **502**, 144187.
18. Y. Yang, G. L. Zhuang, L. M. Sun, X. B. Zhang, X. Q. Yan, W. W. Zhan, X. J. Wang and X. G. Han, *J. Mater. Chem. A*, 2020, **8**, 17449-17453.
19. H. Jung, Y. Whang and S. W. Han, *B. Korean Chem. Soc.*, 2021, **42**, 806-809.
20. X. Wang, W. Li, S. A. He, Q. Ma, B. C. Yan, N. Meng and L. F. Hao, *Int. J. Energy Res.*, 2020, **44**, 833-844.
21. J. F. Wang, P. Fazil, M. I. A. Shah, A. Zada, N. Anwar, G. G. Zain, W. Khan, F. Jan, T. F. Lei and M. Ateeq, *Int. J. Hydrog. Energy*, 2023, **48**, 21674-21685.
22. J. Qin and H. Zeng, *Appl. Catal. B*, 2017, **209**, 161-173.
23. Z. Xu, C. Guo, X. Liu, L. Li, L. Wang, H. Xu, D. Zhang, C. Li, Q. Li and W. Wang, *Chin. J. Catal.*, 2022, **43**, 1360-1370.
24. J. Jiang, Z. Xing, M. Li, Z. Li, J. Yin, J. Kuang, J. Zou, Q. Zhu and W. Zhou, *J. Colloid Interface Sci.*, 2018, **521**, 102-110.
25. M. Li, Z. Xing, J. Jiang, Z. Li, J. Yin, J. Kuang, S. Tan, Q. Zhu and W. Zhou, *J. Taiwan Inst Chem Eng.*, 2018, **82**, 198-204.
26. J. Wang, J. Cong, H. Xu, J. Wang, H. Liu, M. Liang, J. Gao, Q. Ni and J. Yao, *ACS Sustain.*, 2017, **5**, 10633-10639.
27. L.-X. Su, Q. Lou, C.-X. Shan, D.-L. Chen, J.-H. Zang and L.-J. Liu, *Appl. Surf. Sci.*, 2020, **525**, 146576.
28. Q. Zhang, P. Chen, L. Chen, M. Wu, X. Dai, P. Xing, H. Lin, L. Zhao and Y. He, *J. Colloid Interface Sci.*, 2020, **568**, 117-129.
29. Y. Wu, M. Song, Z. Chai and X. Wang, *J. Colloid Interface Sci.*, 2019, **550**, 64-

72.